JOURNAL OF MATERIALS SCIENCE 24 (1989) 599–608

Effect of high rate deformation induced precipitation hardening on the failure of aluminium rivets

VINCENT K. S. CHOO*, PER G. REINHALL, SAEID GHASSAEI
Mechanical Engineering Department, University of Washington, Seattle, Washington, USA

Aluminium alloy (7050-T73) rivets were fabricated by an electromagnetic riveting process. Each rivet was formed in less than 500 μsec. Microcracks and severely deformed regions were observed in the rivet head. Microprobe analysis, optical and scanning electron microscopic examination on the rivets did not yield conclusive evidence that the microcracks were caused by impurities such as iron and silicon. The data obtained in this study support the view that heat generated by material flow at high speed in the rivet head induced precipitation hardening. The precipitation hardening significantly increased the material hardness in the severely deformed shear zone. It is believed that the increment of hardness in the shear zone of the rivets fabricated from the slugs which were previously age hardened resulted in a further decrease in ductility. Hence the initiation of voids which subsequently coalesced to form microcracks in the shear zone.

1. Introduction

An electromagnetic riveting (EMR) process was developed in-house by Boeing Aircraft Company [1]. In this process a rivet was formed from 5/16″ (0.79 cm) Al 7050-T73 slug in less than 500 μsec. Microcracks were found along the well defined shear zone. In this work, an attempt was made to investigate the mechanisms of microcrack formation.

The EMR process induced an extremely high rate of material deformation and large plastic strain. The material response under such extreme conditions was complicated. It has been a subject of intense interest [2–19]. Phase transformation in the severely deformed shear zone was observed [5, 10, 14, 16]. In this study, a finite element analysis and an experimental investigation were conducted. Rivets fabricated by the EMR process were examined by conducting optical and scanning electron microscopy, and microhardness measurement.

Broek [20] has demonstrated that inclusions could serve as sites for the initiation of voids which would grow and coalesce to form microcracks. Furthermore, it was revealed by Senz and Spuhler [21] that impurities such as iron and silicon have a detrimental effect on the toughness of aluminium alloys. In order to ascertain if the microcracks observed were due to impurities, microprobe analysis was also pursued.

2. Analysis

A closed-loop feedback controlled servo-hydraulic testing system (MTS) was used to conduct uniaxial compression tests on 5/16 inch (0.79 cm) 7050-T73 aluminium rivet slugs. The test data indicated that the aluminium slug could be assumed to have elastic-perfectly plastic behaviour. This assumption was adopted for subsequent finite element analysis using DYNA2D [22]. DYNA2D was an explicit axisymmetric finite element program. It was formulated for analysing the dynamic response of solids subjected to large plastic deformation. Sliding with friction along material interfaces was allowed. Modifications of the original DYNA2D program were required to accommodate singularities created by the 90° angles in the rivet-stack geometry and also to prevent unwanted penetration of the stack boundary by the rivet slug. Stacks were the components to be joined by a rivet. Spatial descretization was achieved by using four-node solid brick elements. The equations of motion were integrated explicitly. The EMR process was simulated using the modified DYNA2D. The rivet driver was assumed to weigh 1.4 lb (0.64 kg). Fig. 1 shows the sequence of rivet formation. Though the process took 450 μsec it can be observed that the rivet head was formed fully at about 350 μsec. The simulation of the EMR process was repeated for five other cases with the following die side angles of 50°, 30°, 25°, 20° and 15°. The results of the analysis are shown in Figs 2 and 3. Fig. 2 is a plot of maximum shear stress against rivet die angle. It shows that the maximum shear stress increases with increasing die angle. Fig. 3 shows the variation of interference pressure, at the interface between the rivet shank and stack, with rivet die angle. The maximum interference pressure increases with decreasing die angle.

* *Present address*: Mechanical Engineering Department, New Mexico State University, Box 3450, Las Cruces, New Mexico 88001, USA.

0022–2461/89 $03.00 + .12

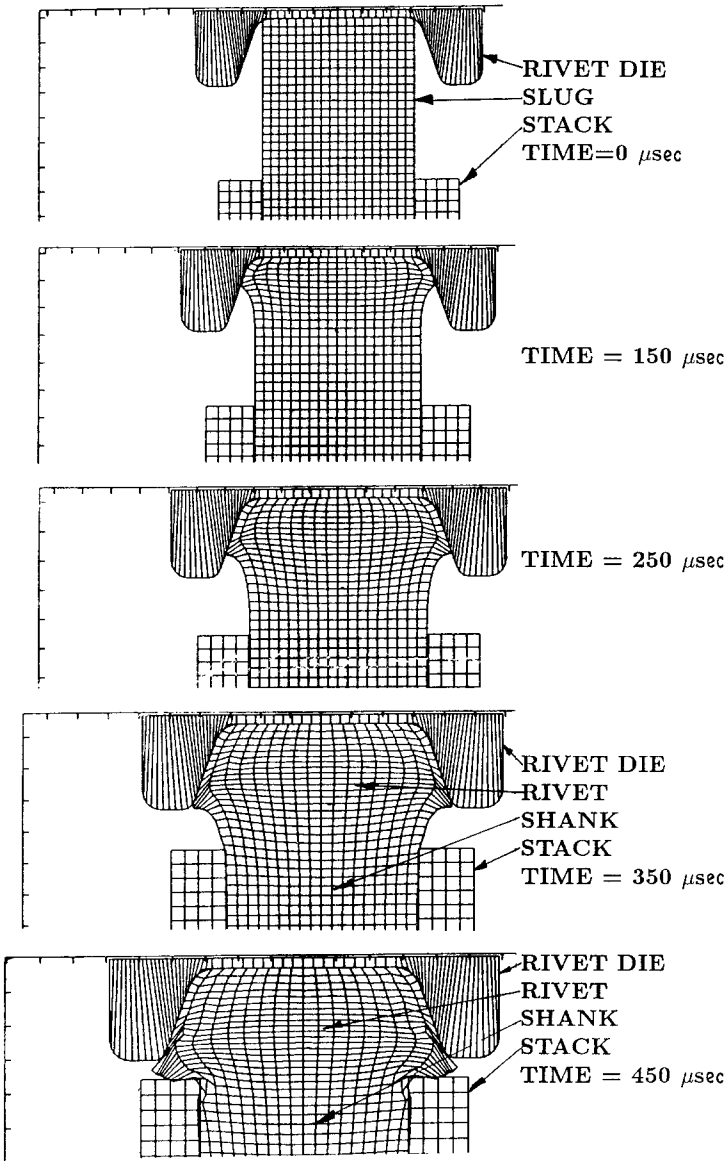

Figure 1 Simulation of rivet formation by the EMR process.

3. Experimentation

Rivet dies with sidewall angles of 40° and 25° were manufactured. These dies were used in conjunction with the EMR machine. Two driver weights of 1.4 lb (0.64 kg) and 5.6 lb (2.56 kg) were employed. The aluminium alloy 7050-T73 rivet slugs were supplied by Alcola. Some of these rivet slugs were solution heat treated again by heating them to 890 ± 10° F (476 ± 5.6° C). This temperature was maintained for 30 min. The slugs were subsequently quenched in cold water. They shall be referred to as solution heat treated rivet slugs in the following presentation. Whereas, the original rivet slugs supplied by Alcola will be referred to as the "as-received rivet slugs". They were age hardened in storage. Rivets were fabricated from both groups of rivet slug. The rivets were sectioned, mounted on potting material, ground, polished and etched for 10 sec using an etchant consisting of the following constituents

(i) 2 ml hydrofloric acid
(ii) 3 ml hydrochloric acid

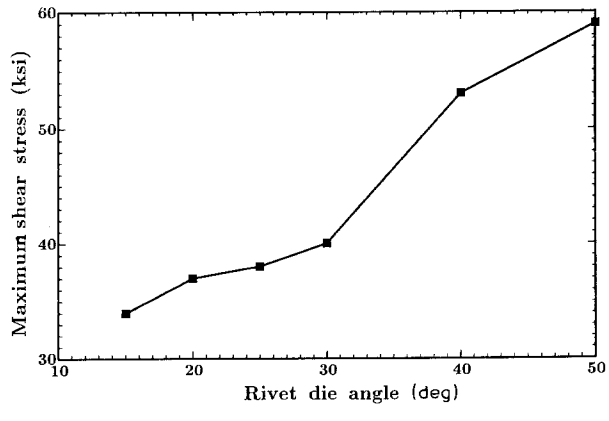

Figure 2 Maximum shear stress as a function of rivet die angle.

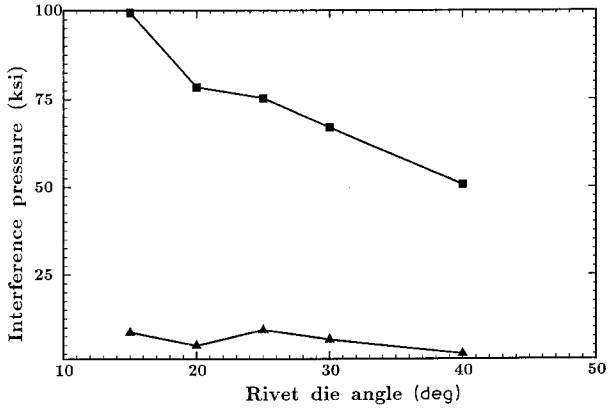

Figure 3 Variation of interference pressure (■ maximum, ▲ minimum) with rivet die angle.

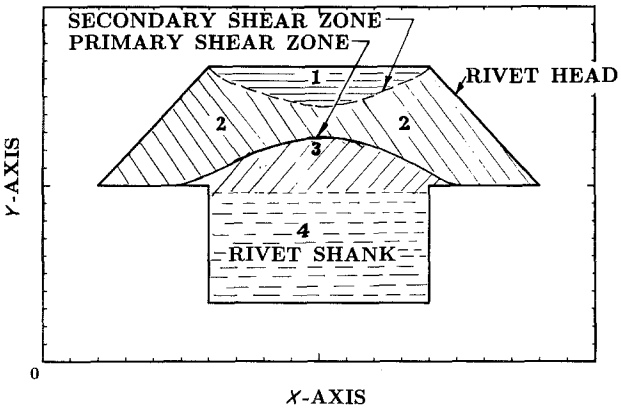

Figure 4 Zoning of a rivet.

(iii) 20 ml nitric acid
(iv) 175 ml water.

Optical microscopy, microprobe analysis and microhardness measurement were conducted. For better visual resolution on the microcracks, some of the polished and etched specimens were coated with a thin layer of gold–palladium and examined using a scanning electron microscope. The results are presented in the following sections.

4. Experimental results

4.1. Optical microscopy

For the sake of convenience a rivet is divided into four regions as shown in Fig. 4. Only the primary shear zone was of significance in this study and the term "primary" will subsequently be dropped when referring to the primary shear zone. The variation of grain size in these regions was examined. Fig. 5 shows variation of grain shapes and sizes. The relative location of the rivet shown in Fig. 5 are illustrated schematically in Fig. 6. Near the top free surface of the rivet head in region 1 the grains were very small and closely packed together. The grains are not elongated in the x direction as defined in Fig. 6. At a small distance below the top free surface the grain increased in size suddenly. The grains remained relatively large for an extended length before decreasing in the size gradually in region 2; but they began to elongate in shape. They aligned themselves and achieved maximum elongation at the shear zone. On the other side of the shear zone in region 3 (see Fig. 6) the grains increased in size very quickly. At a short distance away from the shear zone in region 3, the grains attained sizes comparable to those in the large-grain section of region 1. Fig. 7 is a micrograph of a section of a rivet with relative location shown in Fig. 6. The small grains in region 2 are elongated and orientated along the paths shown in Fig. 6. At the shear zone, grains have elongated extensively. They aligned and orientated themselves parallel to the shear zone. Microcracks found in the shear zone ran parallel to the grains in and near the shear zone. Fig. 8 shows a cross-section perpendicular to the axis of the rivet. The grains in and near the shear zone were stretched circumferentially as shown in Fig. 9 which is a magnified section of Fig. 8. The general appearance of the shear zone created in a rivet formed with 25° die was quite similar to those shown earlier. However, no cracks were found in the shear zone. Fig. 10 shows the shear zone of a rivet formed from the solution heat treated slug with a 40° die. In this case, the shear zone is very diffused. Grain elongation was present but no microcracks were found in the shear zone.

4.2. Scanning electron microscopy

Microcracks in the shear zone are shown clearly in Fig. 11. The coalescence of voids to form microcrack is evident. Some voids were found to contain inclusions. In order to ascertain the material composition of the inclusions, a qualitative X-ray analysis was conducted using the EDAX system. Fig. 12 is the EDAX spectrum of the inclusion. The presence of iron was detected. The EDAX spectrum of a void and inclusion free location in a rivet shank is shown in Fig. 13. No elements of iron could be detected.

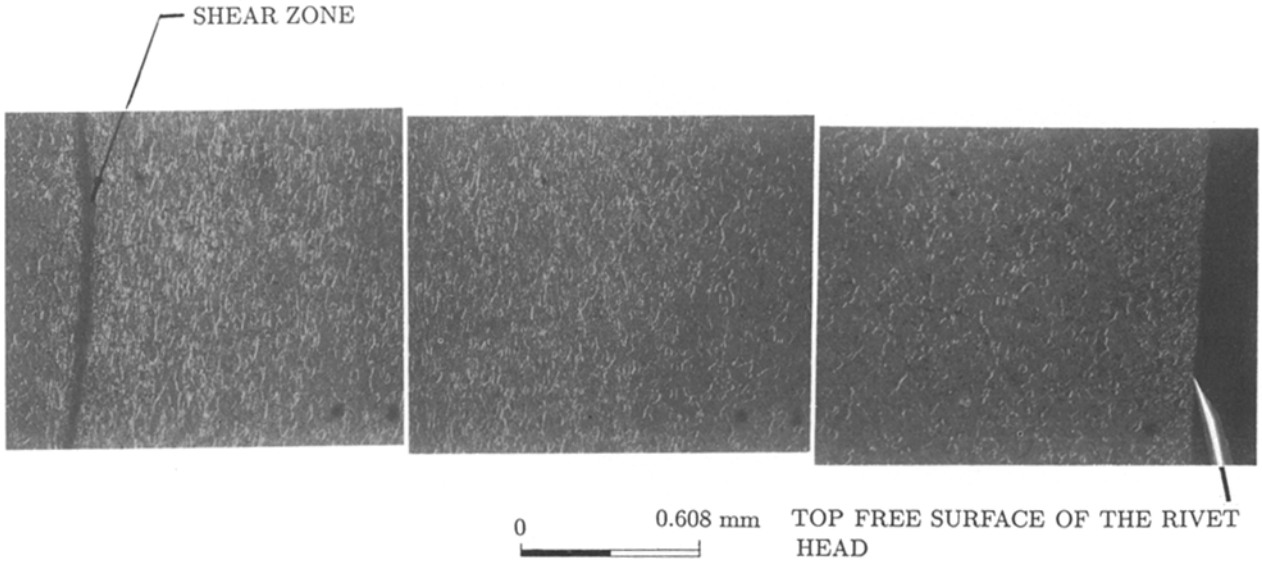

Figure 5 Optical micrograph of a cross-section of a rivet head (Material: as-received 7050-T73, Forming process: EMR, Hammer weight: 1.4 lb (0.64 kg)).

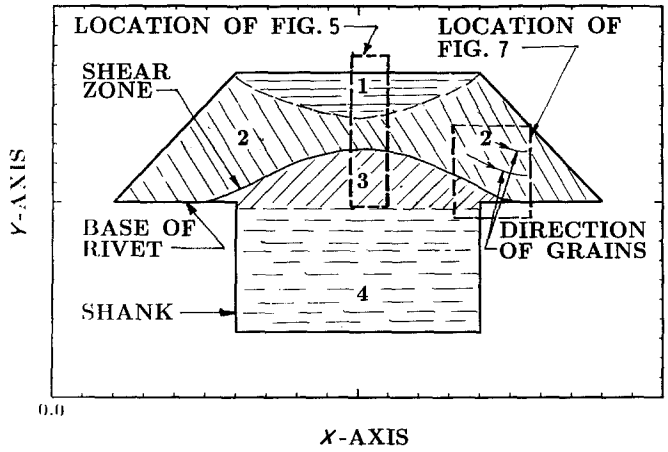

Figure 6 Relative position of Figs 5 and 7.

4.3. Microprobe analysis

The EDAX results prompted a quantitative element analysis. A microprobe was used in this pursuit. The analysis was focussed on the shear zone. X-ray emission spectrograph was conducted. The concentrations of silicon, iron and magnesium were examined. Traces of iron and silicon were found to exist in the rivet. However, further work did not reveal conclusive evidence that these elements were the crack initiation sites.

4.4. Microhardness measurement

The microhardness results obtained are summarized here. Fig. 14 shows the variation of microhardness along the shear zone of a rivet fabricated from the as-received rivet slug using a 40° die. The microhardness on the shear zone was lowest at the centre of the rivet head with a value of about 150 Vickers DPH. The material microhardness increases along the shear zone. It reaches a value of 215 Vickers DPH at point A which is near the base of the rivet head. Rivets fabricated from solution heat treated rivet slugs showed the same trend of microhardness variation along the shear zone as illustrated by Fig. 15. In this case the deformation in the shear zone was very diffuse as evident in Fig. 10. Microhardness also varied across the shear zone. Maximum hardness occurred in the shear zone and tailing off on either side of the shear zone. Such feature is clearly shown in the results obtained from the rivets fabricated using solution heat treated slugs and the 40° die as illustrated in Fig. 16. Only a very small amount of variation in microhardness was observed in the rivet shank.

Rivets fabricated from the as-received slug and 25° die had a small variation of microhardness along the shear zones as can be seen in Fig. 17. The microhardness varies along the shear zone from about 185 Vickers DPH at the base of the rivet head to about 165 Vickers DPH at the centre of the rivet head. At a small distance away from the base of the rivet head, the microhardness along the shear zone approached that in area on either side of the shear zone as shown in Fig. 18.

5. Discussion

Deformation in the rivet was axis-symmetric as can be seen from Fig. 8. Thus the assumption of axis-symmetric deformation made in the DYNA2D program was validated.

Microcracks were found in the shear zones of rivets fabricated by employing the EMR process. The

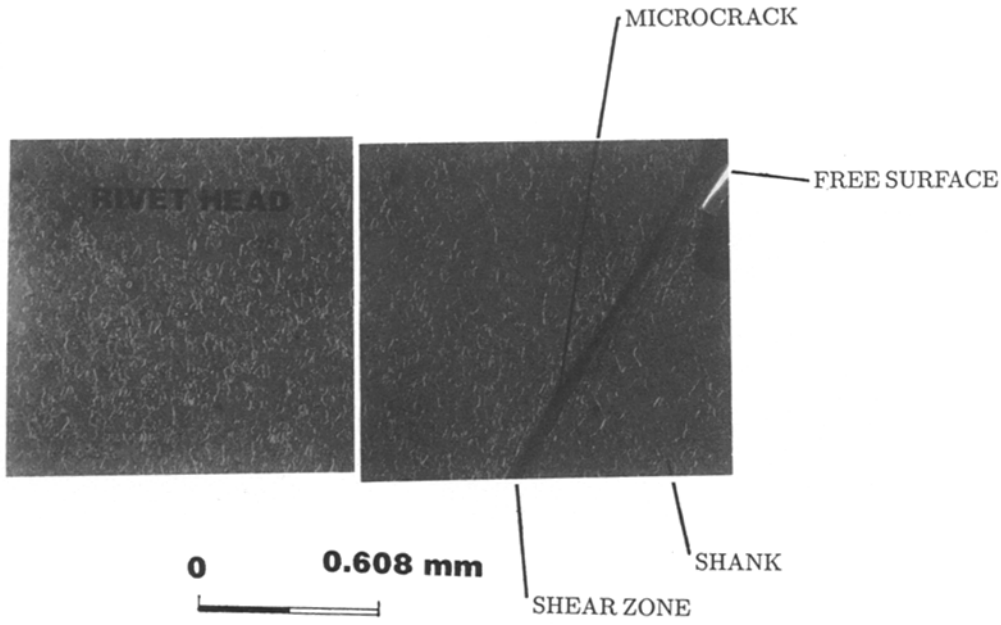

Figure 7 Optical micrograph of a cross-section of a rivet (Material: as-received 7050-T73, Forming process: EMR, Hammer weight 1.4 lb (0.64 kg)).

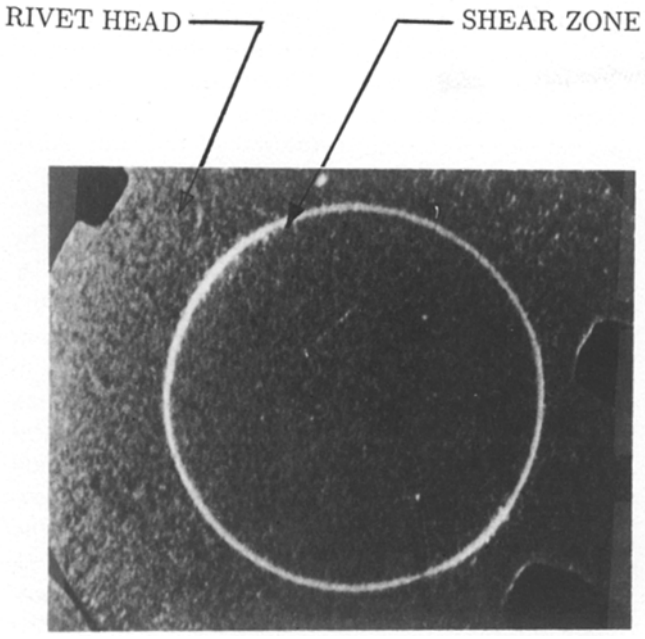

Figure 8 Optical micrograph of cross-section perpendicular to the axis of the rivet (Material: as-received 7050-T73, Forming process: EMR, Hammer weight 1.4 lb (0.64 kg)).

microprobe analysis did not reveal any conclusive evidence that these microcracks were initiated by the presence of impurities such as iron and silicon found. If these impurities had been the cause of microcrack formation, one should still be able to observe these microcracks even in the rivets formed from the solution heat treated rivet slugs, but no such microcracks were observed.

Melellan and Eichenberger [23] have demonstrated that aluminium did exhibit strain hardening behaviour. Associated with the strain hardening was an increase in microhardness and loss in ductility. Rivets fabricated using the same EMR process with different dies would be subjected to the same deformation rate. Therefore, the same degree of strain hardening would be experienced by all the rivets. Hence, the same level of increment in microhardness should occur in all the rivets. However, this did not bear out in the experimental results. Figs 14 and 17 show the microhardness in the shear zone of rivets fabricated using 40° and 25° dies respectively. Both rivets were made from the as-received rivet slugs in the EMR process with a 1.4 lb (0.64 kg) hammer. The 40° rivet possessed a larger increment in microhardness. Therefore, strain hardening could not account for all the loss in ductility experienced by the rivet material when undergoing the high rate of deformation. Strain hardening could occur in the slow hydraulically squeezed rivets formed using the EMR process. Even though strain hardening occurred in all three cases, no microcracks were found in the slow squeezed rivet and the EMR formed 25° rivet fabricated from the as-received slug as well as the 40° EMR formed rivet made of solution heat treated slug. Therefore, it could be concluded that strain hardening did not have a significant effect on the formation of microcracks.

Close packing of grains in the shear zone would increase the microhardness of the material. Nevertheless, it could not explain the difference in microhardness in the shear zones between the 40° and 25° rivets since both have close packing of grains. Furthermore, microhardness varied along the shear zones even though close packing of grains existed throughout the shear zones.

The applied compressive load induced material in region 2 of Fig. 4 to flow in the manner predicted by DYNA2D and observed experimentally. According to the simulation by DYNA2D, no significant grain movement occurred in region 3. This view was supported by the experimental results. Thus the relative grain movement was the highest in the shear zone. Also the relative grain movement increased along the shear zone and attained a maximum level near the base of the rivet head. Friction resulting from such grain movement generated heat which was high along the shear zone and again attained a maximum level

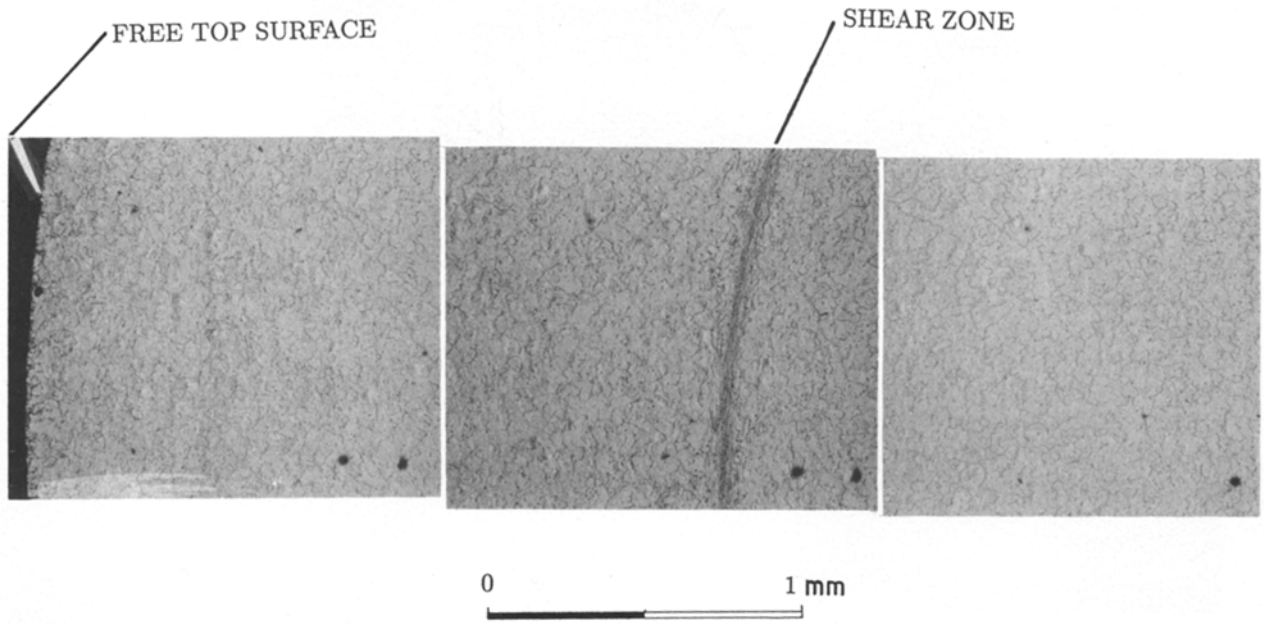

Figure 9 Part of Fig. 8 at a larger magnification.

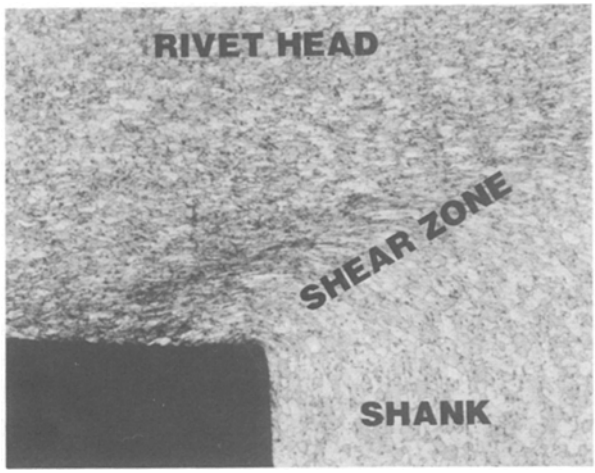

Figure 10 Diffused shear zone created using 40° die and solution heat treated 7050-T73 slug (Forming process: EMR, Hammer weight 1.4 lb (0.64 kg)).

near the base of the rivet head. In the EMR process the rate of heat generation is higher than the rate of heat dissipation. Therefore, a high level of heat could be built up. In contrast heat built-up in the rivet formed by the slow hydraulically squeezed process was unlikely because an equilibrium was always maintained between the heat generation and heat dissipation. The additional increase in microhardness and hence loss in ductility was probably in part due to precipitation hardening. As shown by Reed-Hill [24] the speed at which precipitation takes place depended on temperature. At low temperature, a long period of time were needed for precipitation to complete itself. As the temperature increased, the time required decreased progressively. Therefore, it would be expected that the microhardness in the shear zone would be higher than in the rest of the rivet. Also, microhardness should increase along the shear zone with maximum microhardness occurring near the base of the rivet head. This observation is substantiated by the experimental results shown in Figs 14, 15 and 16.

The solution heat treatment restored the ductility lost as a result of age hardening which was present in the as-received rivet slugs. The shear zones in the rivets formed from the solution heat treated and the as-received slugs were diffused and localized respectively as shown by Figs 10 and 7. This data demonstrated the effect of age hardening. The microhardness results obtained on rivets formed from the solution heat treated rivet slugs as shown in Figs 15 and 16 indicated tentatively that precipitation hardening significantly increased the microhardness in the severely deformed shear zone. This same view had been presented by Grady *et al.* [7]. In addition to the effect of age hardening, the loss in ductility due to precipitation hardening was probably sufficient to cause microcracking in rivets fabricated from the as-received slugs.

Microcracks in the shear zone could be eliminated through inhibiting the temperature built-up and hence suppressing precipitation hardening. Such an objective could be achieved by either reducing the rate of deformation, as was in the case of the slow hydraulically squeezed process, or by decreasing the amount of material flow in the shear zone. The latter was

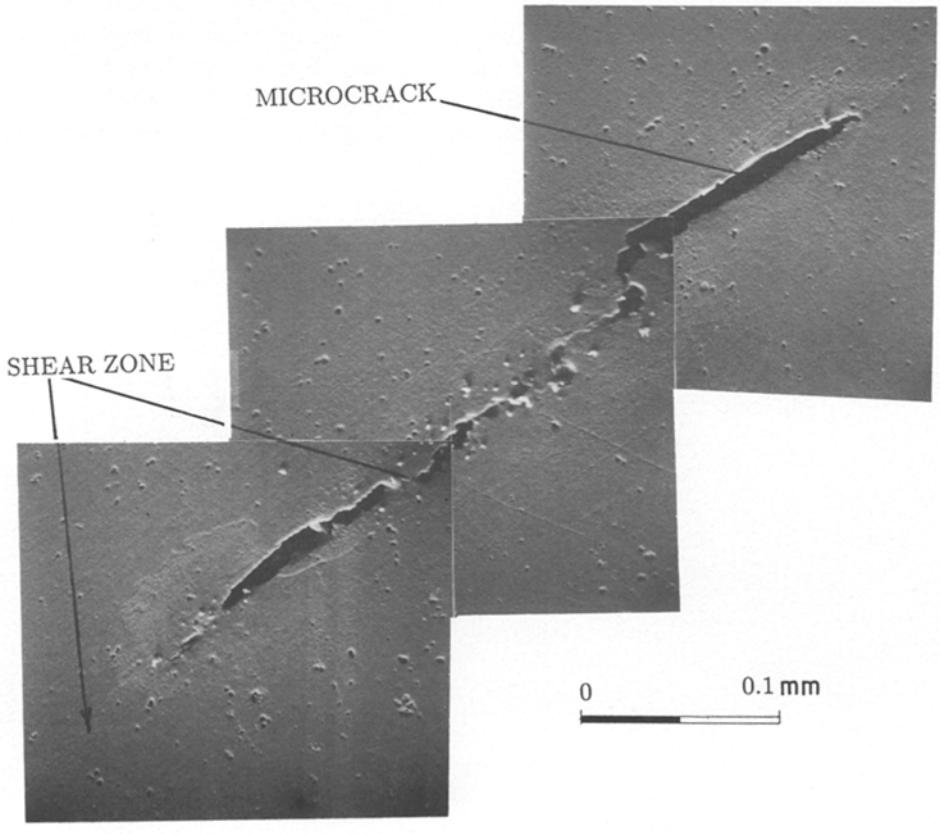

Figure 11 Microcrack in the shear zone.

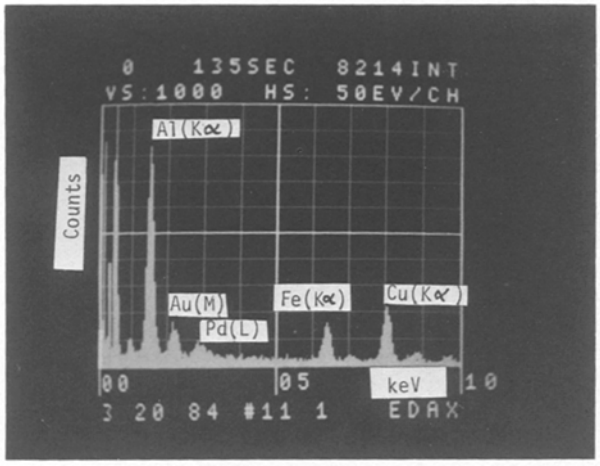

Figure 12 EDX spectrum of the inclusion.

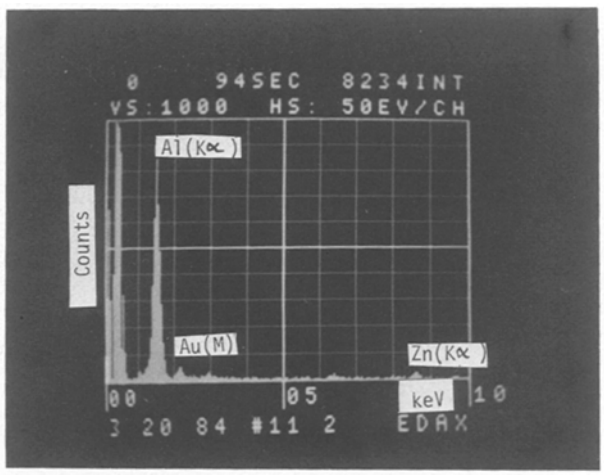

Figure 13 EDX spectrum of a void and inclusion free location in a rivet.

achieved with the aid of 25° die in the EMR process. The subsequent increase in the microhardness of the shear zone was very small as shown in Figs 17 and 18. No microcracks were found in the shear zone even though the rivet was made from the as-received slug with the EMR process. The lower shear stress predicted by the DYNA2D also assisted in the microcrack prevention process.

6. Conclusion

Optical and electron scanning microscopy were conducted on rivets fabricated by employing the EMR process with 40° and 25° dies. Rivets formed from the solution heat treated and the as-received rivet slugs were examined. The material flow characteristics of the rivets were observed to be in agreement with those predicted by the DYNA2D finite element program.

Voids which grew and coalesced to produce microcracks in the shear zone were also observed. Microprobe analysis did not reveal conclusive evidence that the voids were initiated by the presence of impurities such as iron and silicon.

However, the microhardness results obtained on the rivets formed from the solution heat treated slugs indicated a significant increase in microhardness in the severely deformed shear zone. It is believed that the increment was largely due to precipitation hardening. The precipitation hardening phenomenon was made possible by the large amount of heat generated in the shear zone. Such heat generation was due to a large amount of rivet material flow when the rivet was undergoing high deformation rate imparted by the EMR process. No temperature was monitored in the shear zone due to the extreme difficulty. It was construed that the loss in ductility due to age hardening in the as-received slugs and precipitation hardening in

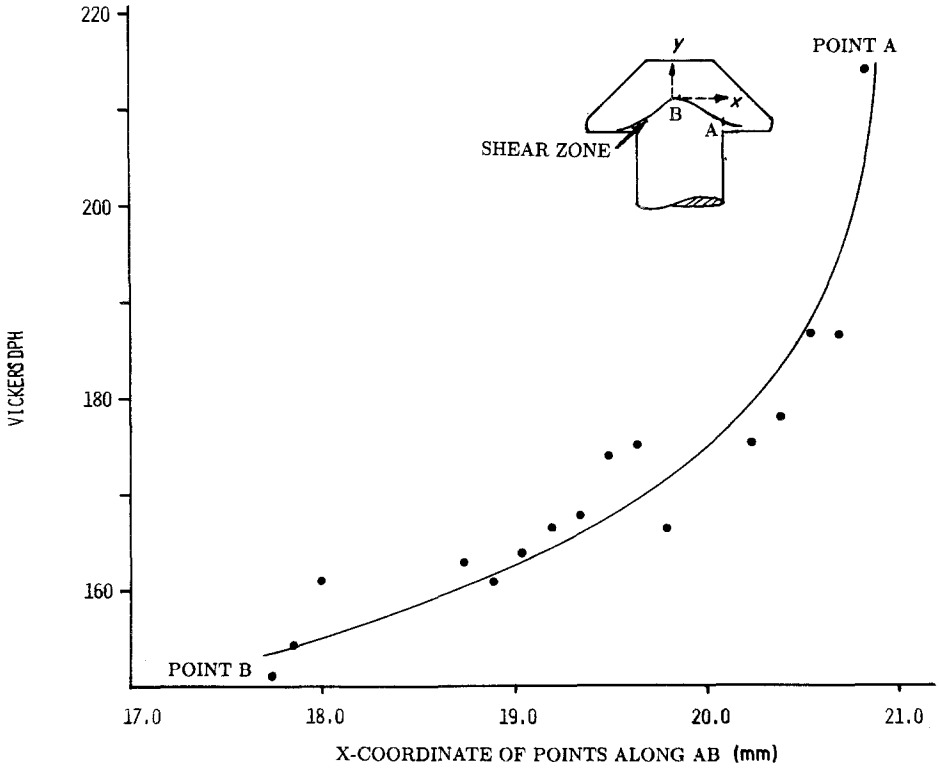

Figure 14 Microhardness variation along the shear zone of a 40° material as-received from Alcola, deformation process EMR shear strength 44 ksi.

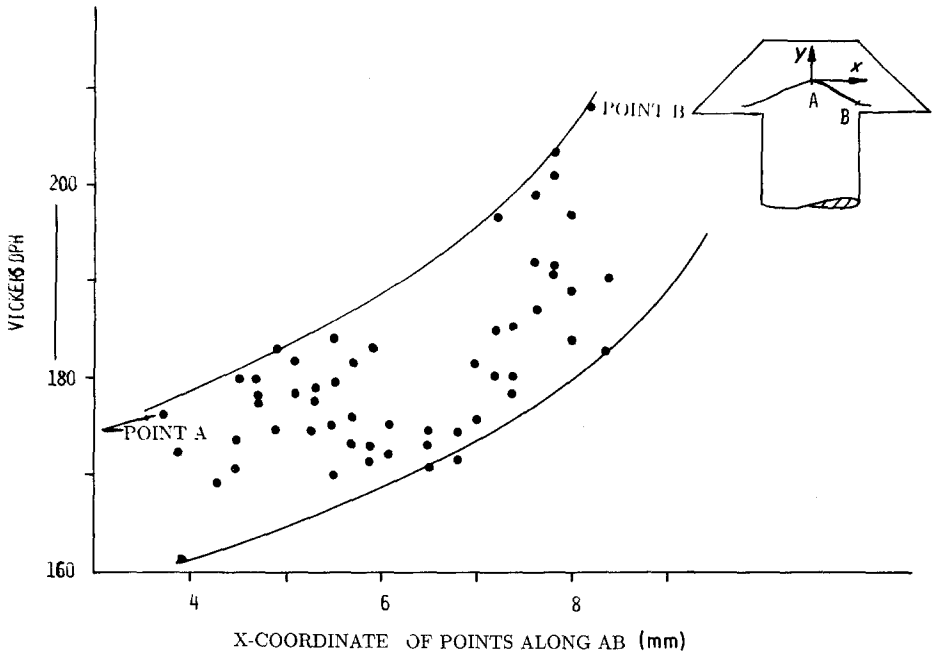

Figure 15 Microhardness variation along the shear zone of a 40° rivet fabricated from solution heat treated slug 7050-T73 deformation process EMR.

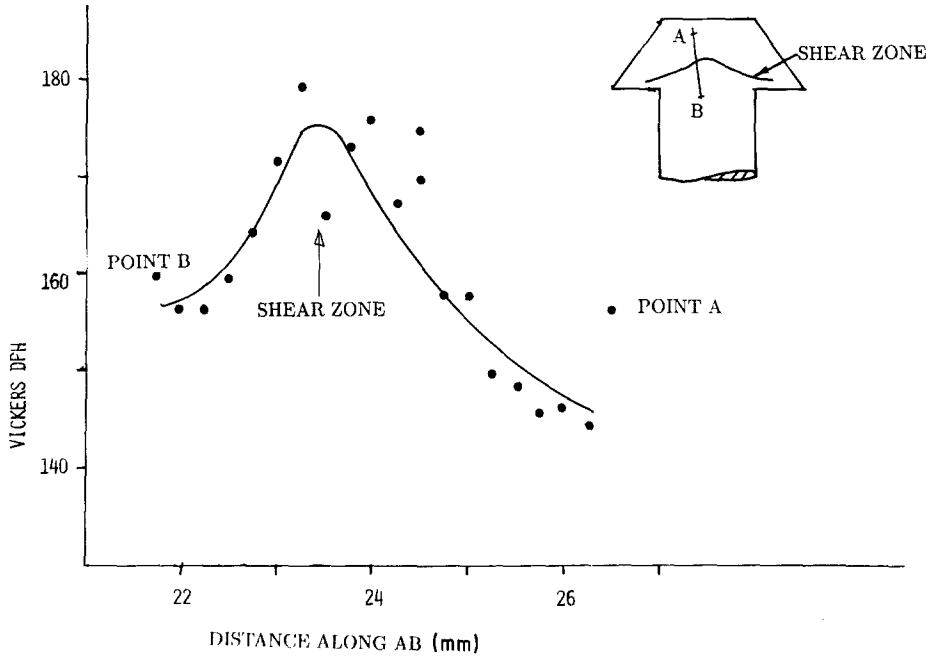

Figure 16 Microhardness variation across the shear zone of a 40° rivet material solution heat treated (7050-T73) EMR deformation process.

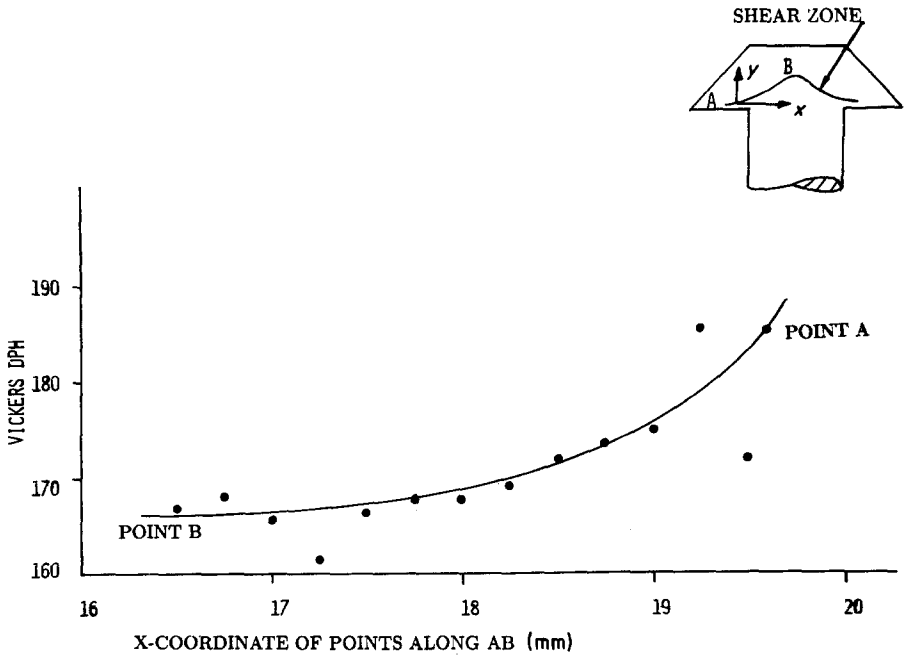

Figure 17 Microhardness variation in the shear zone of a 25° rivet material as-received from Alcola, deformation process EMR shear strength 44 ksi.

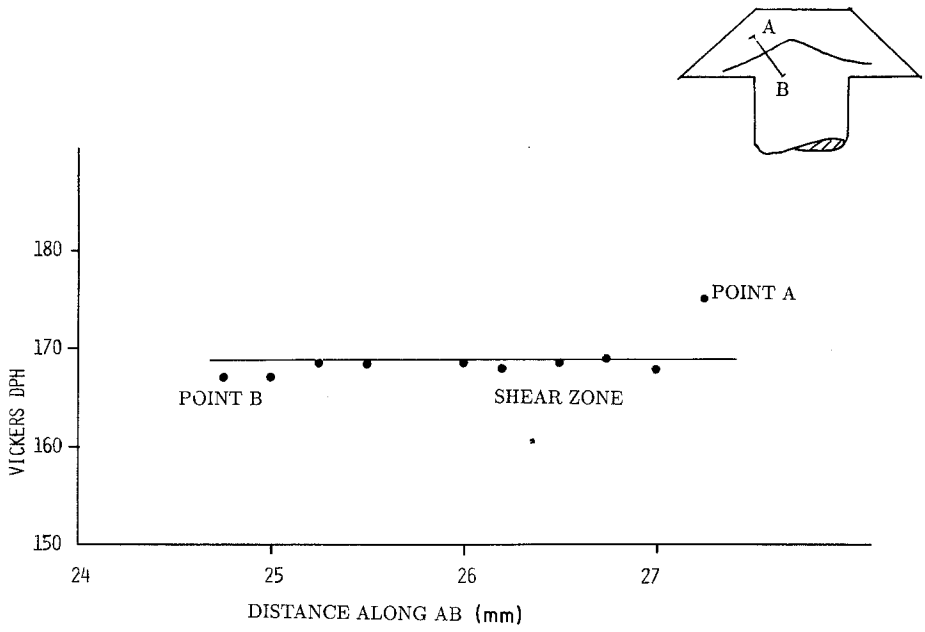

Figure 18 Microhardness variation across the shear zone of a 25° rivet. Material as-received from Alcola, deformation process EMR shear strength 44 ksi.

the shear zone was the cause of microcrack formation in the rivets fabricated from the as-received slugs by the EMR process with a 40° die. Therefore, microcracks in the shear zone could be avoided by preventing precipitation hardening. It was achieved through inhibiting the temperature built-up in the shear zone, either in reducing the rate of load application or by decreasing the amount of material flow in the shear zone.

Acknowledgements

The authors are grateful for the grant provided by Boeing Aircraft Company, Seattle. They acknowledge the assistance provided by the BMT division of Boeing. Thanks are also due to Professor Ed Mathez for his help in the microprobe analysis.

References

1. Electromagnetic Riveting, BCAC Manufacturing Development Report, MDR 6-58021 (1970).
2. C. ZENER and J. H. HOLLOMON, *J. Appl. Phys.* **15** (1944) 22–32.
3. T. A. C. STOCK and K. R. L. THOMPSON, *Metall. Trans.* **1** (1970) 219–224.
4. M. G. STOUT and S. S. HECKER, "Materials Response to Large Plastic Deformation, in Material Behavior Under High Stress and Ultrahigh Loading Rates", edited by J. Mescall and V. Weiss (Plenum Press, New York, 1983) pp. 39–60.
5. H. C. ROGERS, "Adiabatic Plastic Deformation, in Annual Rev., of Materials Science", Vol. 9, edited by R. A. Huggins, R. H. Bube and D. A. Vermilyea (Annual Reviews, Inc., Palo Alto, 1979) pp. 283–311.
6. P. W. BRIDGEMAN, "Studies in Large Plastic Flow and Fracture", McGraw-Hill, New York (1952).
7. D. E. GRADY, J. R. ASAY, R. W. ROHDE and J. L. WISE, " Microstructure and Mechanical Properties of Precipitation Hardened Aluminum Under High Rate Deformation, in Material Behavior Under High Stress and Ultrahigh Loading Rates", edited by J. Mescall and V. Weiss (Plenum, New York, 1983) pp. 81–100.
8. R. A. FRANTZ and J. DUFFY, *J. Appl. Mech.* **39** (1972) 939–945.
9. J. R. ASAY and L. C. CHHABILDAS, "Determination of the Shear Strength of Shock Compressed 6061-T6 Aluminum, in Shock Waves and High Strain-Rate Phenomena in Metals", edited by M. A. Meyers and L. E. Murr (Plenum, New York, 1981) pp. 417–432.
10. H. C. ROGERS, "Adiabatic Shearing – General Nature and Material Aspects, in Material Behavior Under High Stress and Ultrahigh Loading Rates", edited by J. Mescall and V. Weiss (Plenum, New York, 1983) pp. 101–118.
11. R. F. RECHT, *J. Appl. Mech, Trans. ASME* **31E** (1964) 189.
12. S. L. SEMIATIN, G. D. LAHOTI and S. I. OH, "The Occurrence of Shear Bands in Metalworking, in Material Behavior Under High Stress and Ultrahigh Loading Rates", edited by J. Mescall and V. Weiss (Plenum, New York, 1983) pp. 119–160.
13. I. M. HUTCHINGS, "The Behavior of Metals Under Ballistic Impact at Sub-Ordnance Velocities, in Material Behavior Under High Stress and Ultrahigh Loading Rates", edited by J. Mescall and V. Weiss (Plenum, New York, 1983) pp. 161–196.
14. K. P. STAUDHAMMER, C. E. FRANTZ, S. S. HECKER and L. E. MURR, "Effect of Strain Rate on Deformation-Induced Martensite in 304 Stainless Steel, in Shock Waves and High Strain-Rate Phenomena in Metals", edited by M. A. Meyers and L. E. Murr (Plenum, New York, 1981) pp. 91–112.
15. G. B. OLSON, J. F. MESCALL and M. AZRIN "Adiabatic Deformation and Strain Localization, in Shock Waves and High Strain-Rate Phenomena in Metals", edited by M. A. Meyers and L. E. Murr (Plenum, New York, 1981) pp. 221–248.
16. H. C. ROGERS and C. V. SHASTRY "Material Factors in Adiabatic Shearing in Steels, in Shock Waves and High Strain-Rate Phenomena in Metals", edited by M. A. Meyers and L. E. Murr (Plenum, New York, 1981) pp. 285–298.
17. S. M. DORAIVELU, V. GOPINATHAN and V. C. VENKATESH "Formation of Adiabatic Shear Bands During Upsetting of 18-4-1 Alloy Steel at High Strain Rates, in Shock Waves and High Strain-Rate Phenomena in Metals", edited by M. A. Meyers and L. E. Murr (Plenum, New York, 1981) pp. 263–276.
18. G. L. MOSS "Shear Strains, Strain Rates and Temperature Changes in Adiabatic Shear Bands, in Shock Waves and High Strain-Rate Phenomena in Metals", edited by M. A. Meyers, and L. E. Murr (Plenum, New York, 1981) pp. 299–312.
19. C. S. COFFEY and R. W. ARMSTRONG "Description of 'Hot Spots' Associated with Localized Shear Zones in Impact Tests, in Shock Waves and High Strain-Rate Phenomena in Metals", edited by M. A. Meyers and L. E. Murr (Plenum, New York, 1981) pp. 313–324.
20. D. BROEK, *Engng Fract. Mech.* **5** (1973) 55–66.
21. R. R. SENZ and E. H. SPUHLER, *Met. Prog.* (March, 1975) 64–66.

22. User's Manual for DYNA2D, An explicit Two-Dimensional Hydrodynamic Finite Element Code, Lawrence Livermore Laboratory, University of California (January 1984).
23. D. L. MELELLAN and T. W. EICHENBERGER, A "Description of Strain Rate Effects on the Compressive Behavior of Pure Aluminum", Applied Polymer Symposium, no. 5 (Interscience, New York, 1967) pp. 185–201.
24. R. E. REED-HILL, "Physical Metallurgy Principles", Brookes/Cole Engineering Division, Monterrey, CA (1973).

Received 6 January
and accepted 9 May 1988